

Computation of astrophysical opacities*

Claudio Mendoza[†]

Department of Physics, Western Michigan University, Kalamazoo, MI 49008-5252, USA.[‡]

(IPOPv2 Collaboration)

(Dated: April 13, 2017)

The revision of the standard Los Alamos opacities in the 1980-90s by a group at the Livermore Laboratory (OPAL) and the Opacity Project (OP) consortium was an early example of collaborative big-data science, leading to reliable data deliverables (atomic databases, monochromatic opacities, mean opacities and radiative accelerations) that have been widely used since then to solve a variety of important astrophysical problems. Nowadays, the precision of the OPAL and OP opacities, and even that of new tables (OPLIB) by Los Alamos, is a recurrent topic in a hot debate involving stringent comparisons between theory, laboratory experiments, and solar and stellar observations in sophisticated research fields: the Standard Solar Model (SSM); helio and asteroseismology; NLTE 3D hydrodynamic photospheric modeling; nuclear reaction rates, solar neutrino observations, computational atomic physics, and plasma experiments. In this context, an unexpected downward revision of the solar photospheric metal abundances in 2005 spoiled very precise agreement between the helioseismic indicators (depth of the convection zone, sound-speed profile, and helium surface abundance) and the SSM benchmarks, which could be somehow reestablished with a substantial opacity increase. Recent laboratory measurements of the iron opacity in physical conditions similar to the boundary of the solar convection zone have indeed predicted significant increases (30–400%), although new systematic improvements and comparisons of the computational tables have not as yet been able to reproduce them. In the present talk we give an overview of this controversy, and discuss within the OP approach some of the theoretical shortcomings that could be possibly impairing a more complete and accurate opacity accounting.

PACS numbers: 32.70.Cs, 32.70.Jz, 32.80.Aa, 32.80.Fb, 32.80.Hd, 32.80.Zb, 95.30.Ky, 96.60.Fs, 96.60.Jw, 96.60.Ly

I. INTRODUCTION

The *Workshop on Astrophysical Opacities* [1] was held at the IBM Venezuela Scientific Center in Caracas during the week 15–19 July 1991. Although this meeting included several leading researchers concerned with the computation of atomic and molecular opacities, it was essentially a timely encounter between the two teams, namely the Opacity Project (OP) [2] and OPAL [3], that had addressed a 10-year-old plea [4] to revise the Los Alamos Astrophysical Opacity Library (LAAOL) [5]. The mood at the time was jovial because, in spite of the contrasting quantum mechanical frameworks and equations of state implemented by the two groups and the ensuing big-data computations, the general level of agreement of the new Rosseland mean opacities was outstanding.

Further refinements of the opacity data sets carried out the following decade, namely the inclusion of inner-shell contributions by the OP [6], led in fact to improved accord. However, a downward revision of the solar metal abundances in 2005 resulting from NLTE 3D hydrody-

namic simulations of the photosphere [7] disrupted very precise benchmarks in the Standard Solar Model (SSM) with the helioseismic and neutrino-flux predictions [8, 9]. Since then, things have never been the same again.

Independent photospheric hydrodynamic simulations have essentially confirmed the lower metal abundances, specially of the volatiles (C, N, and O) [10]. The opacity increases required to compensate for the abundance corrections have neither been completely matched in extensive revisions of the numerical methods, theoretical approximations, and transition inventories [11–33], nor in a new generation of opacity tables (OPLIB [34]) by Los Alamos [35], nor even in recent innovative opacity experiments [36]. Nonetheless, unexplainable disparities in the modeling of asteroseismic observations of hybrid B-type pulsators with OP and OPAL opacities seem to still question their definitive reliability [37].

In the present talk we give a more detailed overview of this ongoing multidisciplinary discussion, and within the context of the OP approach (IPOPv2), analyse some of the theoretical shortcomings that could be possibly impairing a more complete and accurate opacity accounting. In particular, we discuss spectator-electron processes responsible for the broad and asymmetric resonances arising from core photoexcitation, K-shell resonance widths, and ionization edges since it has been recently shown that the solar opacity profile is sensitive to the Stark broadening of K lines [29].

* This review is based on a talk given at the 12th International Colloquium on Atomic Spectra and Oscillator Strengths for Astrophysical and Laboratory Plasmas, Sao Paulo, Brazil, July 2016.

[†] Also Emeritus Research Fellow, Venezuelan Institute for Scientific Research.

[‡] claudio.mendozaguardia@wmich.edu

II. OP AND OPAL PROJECTS

A. Numerical methods

In the computations of the atomic data required for opacity estimates—namely level energies, f -values, and photoionization cross sections—OP and OPAL used markedly different quantum-mechanical methods. The former adopted a multichannel framework based on the close-coupling expansion of scattering theory [38], where the $\Psi(SL\pi)$ wave function of an $(N+1)$ -electron system is expanded in terms of the N -electron χ_i core eigenfunctions

$$\Psi(SL\pi) = \sum_i \chi_i \theta_i + \sum_j c_j \Phi_j(SL\pi). \quad (1)$$

The second term in Eq. (1) is a configuration-interaction (CI) expansion built up from core orbitals to account for orthogonality conditions and to improve short-term correlations. Core orbitals were generated with standard CI atomic structure codes such as SUPERSTRUCTURE [39] and CIV3 [40], and the total system wave functions and radiative data were computed with the R -matrix method [41, 42] including extensive developments in the asymptotic region specially tailored for the project [43]. The latter allowed the treatment of both the discrete and continuum spectra for an ionic species in a unified manner (see Fig. 1), its effectiveness depending on the accuracy and completeness of the core eigenfunction expansion in Eq. (1), particularly at the several level crossings that take place along an isoelectronic sequence as the atomic number Z increases.

The OPAL code, on the other hand, relied on parametric potentials that generated radiative data of accuracy comparable to single-configuration, self-consistent-field, relativistic schemes [44, 45]. The parent (i.e. core) configuration defines a Yukawa-type potential

$$V = -\frac{2}{r} \left((Z-v) + \sum_{n=1}^{n_{\max}} N_n \exp(-\alpha_n r) \right) \quad (2)$$

with $v = \sum_{n=1}^{n_{\max}} N_n$ for all the subshells and scattering states available to the active electron. In Eq. (2), N_n is the number of electrons in the shell with principal quantum number n , n_{\max} being its maximum value in the parent configuration, and α_n are n -shell screening parameters determined from matches of solutions of the Dirac equation with spectroscopic one-electron, configuration-averaged ionization energies. Thus, in this approach the atomic data were computed on the fly as required rather than relying on stored files (as in OP) that might prove inadequate in certain plasma conditions.

B. Equation of state

The formalisms of the equation of state implemented by OP and OPAL were also significantly different. In

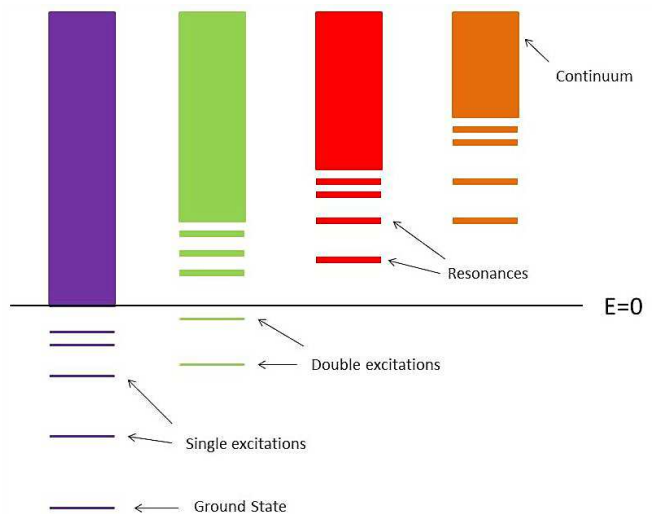


FIG. 1. Multichannel ionic structure showing series of singly and doubly excited bound states and resonances and several continua.

the OP the chemical picture was emphasized [46, 47], where clusters (i.e. atoms or ions) of fundamental particles can be identified and the partition function of the canonical ensemble is factorizable. Thermodynamic equilibrium occurs when the Helmholtz free energy reaches a minimum for variations of the ion densities, and the internal partition function for an ionic species s can then be written

$$Z_s = \sum_i w_{is} g_{is} \exp(-E_{is}/kT) \quad (3)$$

where g_{is} and w_{is} are respectively the statistical weight and occupation probability of the i th level. The main problem was then the estimate of the latter which was performed assuming a nearest-neighbor approximation for the ion microfield or by means of distribution functions that included plasma correlation effects.

In OPAL the equation of state was based on many-body activity expansions of the grand canonical partition function that avoided Helmholtz free-energy compartmentalization [48]. Since pure Coulomb interactions between the electrons and nuclei are assumed, the divergence of the partition function does not take place, and thus there is no need to consider explicitly the plasma screening effects on the bound states.

C. Revised opacities

When compared to the LAAOL (see Fig. 2), preliminary OPAL iron monochromatic opacities at density $\rho = 6.82 \times 10^{-5} \text{ g cm}^{-3}$ and temperature $T = 20 \text{ eV}$ indicated large enhancements at photon energies around 60 eV [49]. They are due to an $n = 3 \rightarrow 3$ unresolved transition array that significantly enhances the Rosseland mean since its average function peaks at around

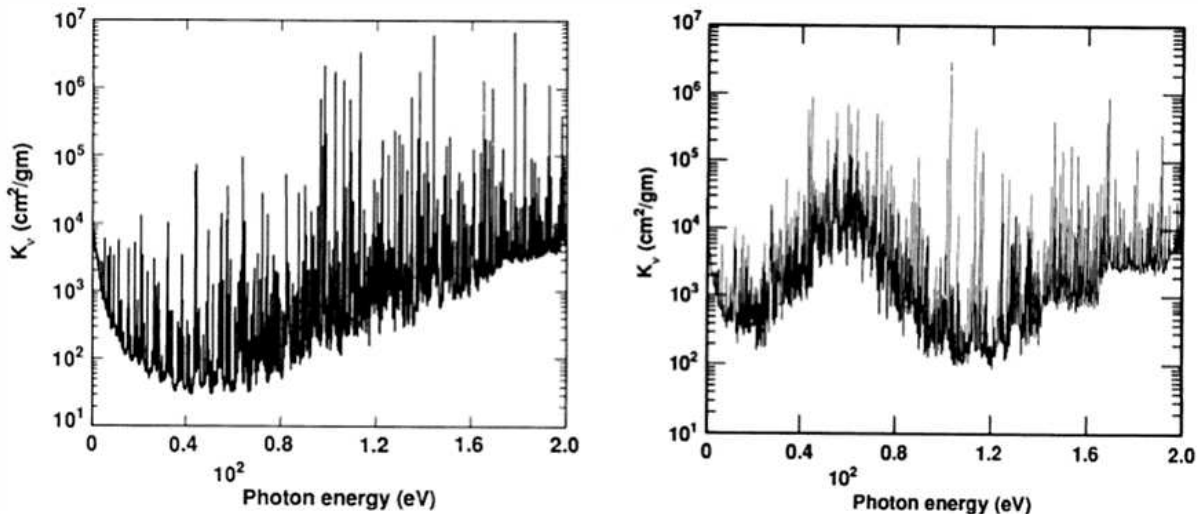


FIG. 2. Monochromatic Fe opacities at $\rho = 6.82 \times 10^{-5} \text{ g cm}^{-3}$ and $T = 20 \text{ eV}$. Left panel: LAAOL. Right panel: OPAL. Reproduced from Figs. 1-2 of Ref. [49] with permission of the ©AAS and the Lawrence Livermore National Laboratory.

80 eV. Within the OP *R*-matrix approach, such transitions were computationally intractable at the time, and were then treated for the systems Fe VIII to Fe XIII in a simpler CI approach (i.e. second term of Eq. 1) with the SUPERSTRUCTURE atomic structure code [50]. The dominance of this Δn unresolved transition array in Fe was subsequently verified by laboratory photoabsorption measurements [51].

It was later pointed out that, in spite of general satisfactory agreement, the larger differences between the OPAL and OP opacities were at high temperatures and densities due to missing inner-shell contributions in OP [52]. Hence, the latter were systematically included in a similar CI approach with the AUTOSTRUCTURE code

in what became a major updating of the OP data sets [6, 53, 54] that can be gauged in Fig. 3 for the solar S92 mix. After this effort and as can be appreciated in Fig. 4, the OPAL and OP opacities were thought to be in good working order, and it was actually mentioned that they could not be differentiated in stellar pulsation calculations [55].

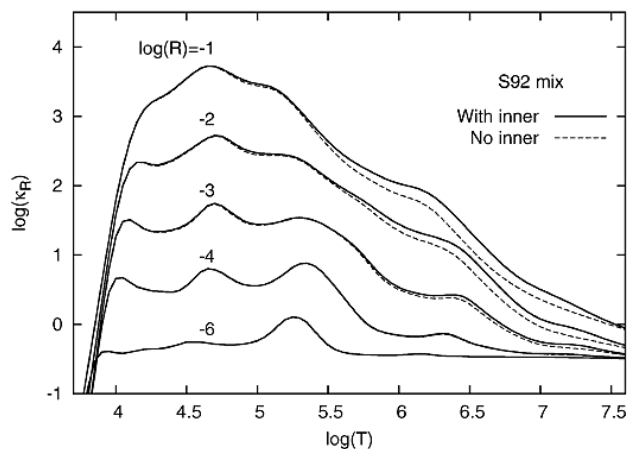


FIG. 3. Inner-shell contributions to the Rosseland-mean opacities for the S92 mix. Note: $R = \rho/T_6^3$ where ρ is the mass density in g cm^{-3} and $T_6 = 10^{-6} \times T$ with T in K. Reproduced from Fig. 1 of Ref. [6].

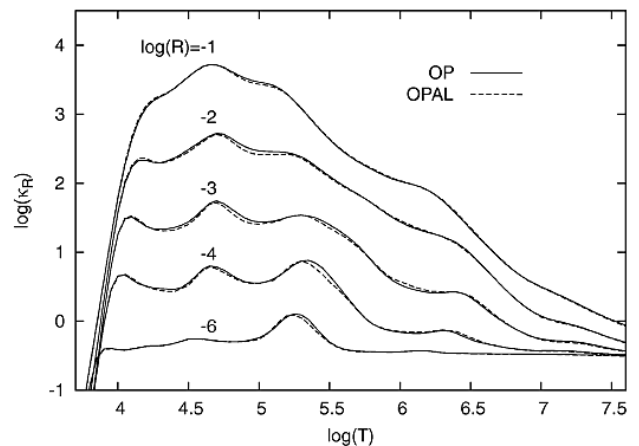


FIG. 4. Comparison of the OP and OPAL Rosseland-mean opacities for the S92 mix. Reproduced from Fig. 2 of Ref. [6].

D. Big-data science

The OP was a pioneering example of what are now called collaborative big-data science projects [56]. It involved the computation of large data sets by several internationally distributed research groups, which were then compiled and stringently revised before becoming part of

what eventually became TOPbase [57, 58], one of the first online atomic databases. In order to ensure machine independence, its database management system was completely developed from scratch in standard Fortran-77, and its user interface rapidly evolved from command based to web-browser based. Furthermore, TOPbase was housed right from the outset in a *data center*, namely the Centre de Données astronomiques de Strasbourg (CDS) [59], also a seminal initiative at the time.

Regarding the dissemination of monochromatic and mean opacities for arbitrary chemical mixes, the OP also implemented the innovative concept of a *web service*, namely the OPserver [60], accessible online from the Ohio Supercomputer Center [61]. Since the main overhead in the calculation of mean opacities or radiative accelerations is the time taken to read large data volumes from secondary storage (disk), the OPserver always keeps the bulk of the monochromatic opacities in main memory (RAM) waiting for a service call from a web portal or the modeling code of a remote user; furthermore, the OPserver can also be downloaded (data and software) to be installed locally in a workstation. Its current implementation and performance are tuned up to support stellar structure or evolution models requiring mean opacities for varying chemical mixtures to be determined at every radial point or time interval.

III. SOLAR ABUNDANCE PROBLEM

A. Standard Solar Model

In 2005 there was much expectation in the solar modeling community for the OP inner-shell opacity update (see Section II C) as the very precise and much coveted benchmarks of the Standard Solar Model (SSM) with the helioseismic indicators—namely the depth of the convection zone, He surface abundance, and sound-speed profile—had been seriously disrupted by a downward revision of the photospheric metal abundances [7]. The latter was the result of advanced 3D hydrodynamic simulations that took into account granulation and NLTE effects [8, 9]. In this regard, the final improved agreement between the OP and OPAL mean opacities after the aforementioned update turned out to be a disappointment in the SSM community.

This situation can be appreciated in Table I where the SSM benchmarks with the helioseismology measurements of the convection-zone depth and He surface mass fraction are hardly modified by the opacity choice (OPAL or OP), while the new abundances [7] lead to noticeable modifications. It is further characterized by the SSM discrepancies with the helioseismology sound-speed profile near the base of the convection zone (see Fig. 5), which has been shown to disappear with an opacity increase of $\sim 30\%$ in this region down to a few percent in the solar core [62].

TABLE I. SSM benchmarks (BS05 model from [9]) with the helioseismic predictions [63], namely the depth of the convection zone (R_{cz}/R_{sun}) and He surface mass fraction (Y_{sur}), using OP and OPAL opacities and the standard (GS98) [64] and revised (AGS05) [7] metal abundances.

Model	R_{cz}/R_{sun}	Y_{sur}
BS05(GS98,OPAL)	0.715	0.244
BS05(GS98,OP)	0.714	0.243
BS05(AGS05,OPAL)	0.729	0.230
BS05(AGS05,OP)	0.728	0.229
Helioseismology	0.713(1)	0.249(3)

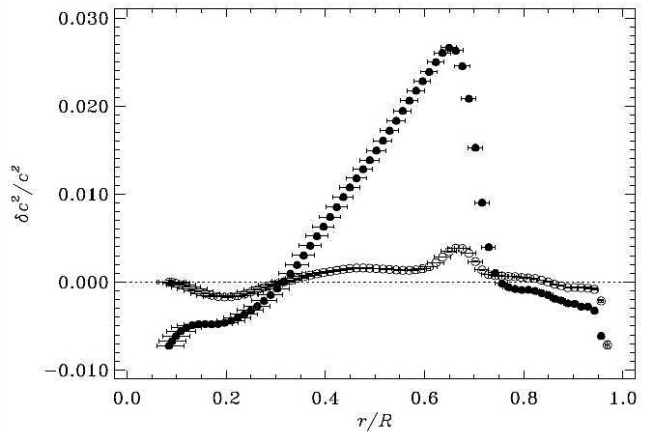


FIG. 5. Relative sound-speed differences between helioseismic measurements and SSM. Open circles: using the standard solar composition [64]. Filled circles: using the revised metal abundances [7]. Reproduced from Fig. 1 of Ref. [62] with permission of \odot ESO.

B. Seismic Solar Model

The sound-speed profile in the solar core has also been useful, in what is referred to as the Seismic Solar Model (SeSM) [65], in verifying the reliability of the highly temperature-dependent (and thus opacity-dependent) nuclear reaction rates in reproducing the observed solar neutrino fluxes. In other words, both the helioseismic indicators and neutrino fluxes become fairly strict constraints on the opacities and metal abundances (both of volatile and refractory elements) at different solar radii. For instance, the higher metallicity recently derived from *in situ* measurements of the solar wind [66] (see Table II) has been seriously questioned [67] in spite of improved accord with helioseismology because of a neutrino overproduction caused by the refractory excess (i.e. from Mg, Si, S, and Fe). In Table II a more recent revision of the photospheric metallicity [68] is also tabulated that is $\sim 10\%$ higher but still $\sim 25\%$ lower than the previously assumed standard [64], and which has been independently confirmed by a similar 3D hydrodynamic approach [10]. It has been shown [69] that, with the more

TABLE II. Solar abundances ($\log \epsilon_i \equiv \log N_i/N_H + 12$). GS98: Ref. [64]. AGS05: Ref. [7]. AGSS09: Ref. [68]. CLSFB11: Ref. [10]. SZ16: Ref. [66].

i	GS98	AGS05	AGSS09	CLSFB11	SZ16
C	8.52	8.39(5)	8.43(5)	8.50(6)	8.65(11)
N	7.92	7.78(6)	7.83(5)	7.86(12)	7.97(15)
O	8.83	8.66(5)	8.69(5)	8.76(7)	8.82(10)
Ne	8.08	7.84(6)	7.93(10)		7.79(17)
Mg	7.58	7.53(9)	7.60(4)		7.85(17)
Si	7.56	7.51(4)	7.51(3)		7.82(18)
S	7.20	7.14(5)	7.12(3)	7.16(5)	7.56(19)
Fe	7.50	7.45(5)	7.50(4)	7.52(6)	7.73(17)
Z/X	0.0229	0.0165	0.0181	0.0209	0.0265

recent abundances of [68], the required opacity increase in the SSM to restore the helioseismic benchmarks is only now around 15% at the base of the convection zone and 5% in the core, i.e. half of what was previously estimated [62].

C. Multidisciplinary approach

Consensus has been reached in a multidisciplinary community encompassing sophisticated research fields (see Fig. 6), wherein the computation and measurement of opacities have leading roles, that there is at present a solar abundance problem. This critical situation is encouraging further developments and discussions that, in a similar manner to the solar neutrino problem, are expected to converge soon to a satisfying solution. For instance, since the SSM is basically a static representation,

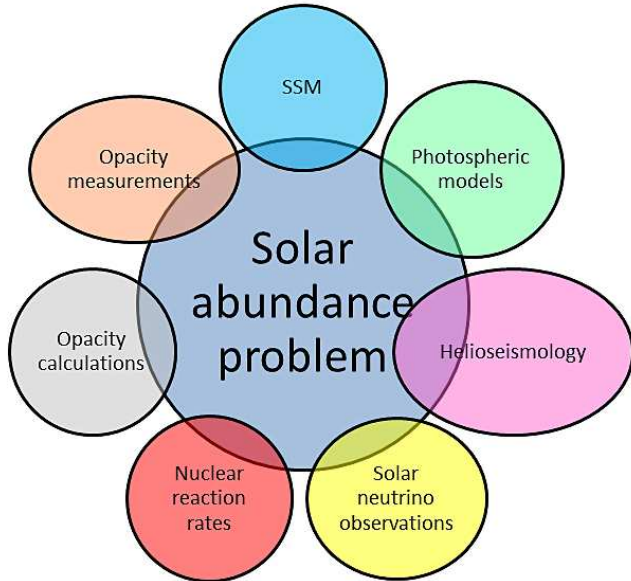


FIG. 6. Research fields of the multidisciplinary community involved in the solar abundance problem.

there has been renewed interest in considering magnetic and dynamical effects such as rotation, elemental diffusion and mixing, and convection overshoot [65, 70]. Nuclear fusion cross sections have also been critically evaluated pinpointing cases for which the current precision could be improved [71].

Helioseismology has become a very powerful diagnostic technique; for instance, it remarkably enables the performance evaluation of the different equations of state [72], and with the advent of the *Kepler* [73] and *CoRoT* [74] space probes, it has been successfully applied to other stellar structures and evolutionary models in what is rapidly becoming a new well-established research endeavor: asteroseismology [75]. In this regard it has been curiously shown that, in the complex asteroseismology of some hybrid B-type pulsators (e.g. γ Pegasi), both OPAL and OP opacity tables perform satisfactorily [76], but in others, namely ν Eridani, inconsistencies appear in the analysis that still seem to indicate missing opacity [37], a point that is treated to some extent in Sections IV–V.

IV. OPACITIES, RECENT DEVELOPMENTS

In a similar way to other research areas of Fig. 6, the solar abundance problem has stimulated detailed revisions and new developments of the astrophysical opacity tables and the difficult laboratory reproduction of the plasma conditions of the solar convection zone so as to obtain comparable measurements.

The OPAC international consortium [16, 19] has been carrying out extensive comparisons using a battery of opacity codes (SCO, CASSANDRA, STA, OPAS, LEDCOP, OP, and SCO-RCG), looking into the importance of configuration interaction and accounting mainly in elements of the iron-group bump (Z bump), i.e. Cr, Fe, and Ni, due to their relevance in the pulsation of intermediate-mass stars. Problems with both the OPAL and OP tables have been reported; for instance, there are considerable differences in the OPAC and OP single-element monochromatic opacities although OPAC Rosseland mean opacities for a solar mixture agree fairly well with both OPAL and OP [15].

A new generation of Los Alamos opacity tables (OPLIB) including elements with atomic number $Z \leq 30$ have been computed with the ATOMIC code and made publicly available [35]. They have been used to study the Z bump, finding reasonable agreement with transmission measurements in the XUV but factors of difference with the OP Rosseland-mean tables for Fe and Ni [33]. Also, relativistic opacities for Fe and Ni computed with the Los Alamos codes are found to be in good agreement with semi-relativistic versions providing confidence in the numerical methods [23].

Solar models have been recently computed with both the OPLIB and OPAL opacity tables and the metal abundances of [68], finding only small differences in the helioseismic indicators although the OPLIB data display

steeper opacity derivatives at the temperatures and densities associated with the solar interior [77]. These opacity derivatives directly impact stellar pulsation properties such as the driving frequency, and since the latter data set has also been shown to yield a higher Rosseland mean than OPAL and OP in the Z-bump region, it gives rise to wider B-type-pulsator instability domains [78]. However, basic pulsating star problems remain unsolved such as the pulsations of the B-type stars in the Large and Small Magellanic Clouds. Moreover, in a recent analysis of the oscillation spectrum of ν Eridani with different opacity tables, OPLIB is to be preferred over OPAL and OP, but the observed frequency ranges can only be modeled with substantially modified mean-opacity profiles that are nevertheless impaired by puzzling side effects [79].

The OPAL opacity code has been updated (now referred to as TOPAZ) to improve atomic data accuracy and used to recompute the monochromatic opacities of the iron-group elements [24]; small decreases (less than 6%) with respect to the OPAL96 tables have been found. The OP collaboration (IPOPv2), on the other hand, has been performing test calculations on the Ni opacity by treating Ni XIV as a study case [18], and a new online service for generating opacity tables is now available [80].

To bypass the computational shortcomings of the detailed-line-accounting methods in managing the huge number of spectral lines of the more complex ions, novel methods based on variations and extensions of the Unresolved-Transition-Array (UTA) concept [81] have been implemented. In these methods, the transition array between two configurations is usually reduced to a single Gaussian, but can be replaced by a sum of partially resolved transition arrays represented by Gaussians [82, 83] that are then sampled statistically to simulate detailed line accounting [84]. For heavy ions where UTAs still fall short, a higher-level extension referred to as the Super-Transition-Array (STA) method involves the grouping of many configurations into a single superconfiguration, whereby the UTA summation to a single STA can be performed analytically [85–87]. Recent STA calculations of the Rosseland mean opacities in the solar convection zone boundary agree very well with both OP and OPAL, and predict a meagre heavy-element ($Z > 28$) contribution [28].

The most salient effort has perhaps been the recent measurements of Fe monochromatic opacities in laboratory plasma conditions similar to the solar convection zone boundary ($T_e = 1.9\text{--}2.3$ MK and $n_e = 0.7\text{--}4.0 \times 10^{22} \text{ cm}^{-3}$) that show increases (30–400%) that have not as yet been possible to match theoretically [36]. However, the mean-opacity enhancements are still not large enough (only 50%) to restore the SSM helioseismic benchmarks, but sizeable experimental increases in other elements of the solar mixture such as Cr and Ni would certainly reduce the current discrepancy. Furthermore, a point of concern in this experiment is the model dependency of the electron temperature and density determined by K-

shell spectroscopy of tracer Mg, but as discussed in [88], it is not expected to be large enough to explain the discord with theory.

The line broadening approximations implemented in most opacity calculations have been recently questioned [29], reporting large discrepancies between the OP K-line widths and those in other opacity codes. It is therein also shown that the solar opacity profile is sensitive to the pressure broadening of K lines, which can be empirically matched with the helioseismic indicators by a K-line width increase of around a factor of 100. However, the line-broadening dependency of the solar opacity near the bottom of the convection zone has been previously reported only as moderate, i.e. to within a few percent [54, 89], and thus this new finding only seems to reconfirm it.

A. Fe opacity

The iron opacity is without a doubt the most revered in the atomic astrophysics context due, on the one hand, to its relevance in the structure of the the solar interior and the driving of stellar pulsations, and on the other, to the difficulties in obtaining accurate and complete radiative data sets for the Fe ions. In this respect, the versatile HULLAC relativistic code [90] has been used to study CI effects mainly in $3 \rightarrow 3$ and $3 \rightarrow 4$ transitions that dominate the maximum of the Rosseland mean [21]. At $T = 27.3$ eV and $\rho = 3.4 \text{ mg cm}^{-3}$, it is found that CI causes noticeable changes in the spectrum shape by line shifts at the lower photon energies; good agreement is found with OP in contrast to the spectra by other codes such as SCO-RCG, LEDCOP, and OPAS. The importance of CI is also brought out in comparisons of the OP and OPAL monochromatic opacities with old transmission measurements, namely spectral energy displacements [21]. However, a further comparison [33] with recent results at $T = 15.3$ eV and $\rho = 5.48 \text{ mg cm}^{-3}$ obtained with the ATOMIC modeling code, which include contributions from transitions with $n \leq 5$, shows significantly higher monochromatic opacities than OP for photon energies greater than 100 eV and almost a factor of 2 increase in the Rosseland mean; it is therein pointed out that this is due to limited M-shell configuration expansions in OP for ions such as Fe VIII.

A more controversial situation involves the recently measured Fe monochromatic opacities that proved to be higher than expected in conditions similar to the solar convection zone [36]. Such a result came indeed as a surprise since previous comparisons of transmission measurements at $T = 156 \pm 6$ eV and $N_e = 6.9 \pm 1.7 \times 10^{21} \text{ cm}^{-3}$ with opacity models—namely ATOMIC, MUTA, OPAL, PRIMSPECT, and TOPAZ—showed satisfying line-by-line agreement [35, 91, 92]. Relative to [36], the OP values are not only lower but the wavelengths of the strong spectral features are not reproduced accurately. Other codes, namely ATOMIC, OPAS,

SCO-RCG, and TOPAZ, perform somewhat better regarding the positions of the spectral features but the absolute backgrounds are also generally too low; moreover, the computed Rosseland means are in general smaller than experiment by factors greater than 1.5. It has been suggested that calculations have missing bound-bound transitions or underestimate some photoionization cross sections [36]. The measured windows are higher than those predicted by the models, the peak values show a large (50%) scatter, and the measured widths of prominent lines are significantly broader. On the other hand, from the point of view of oscillator-strength distributions and sum rules, the measured data appear to display unexplainable anomalies [92].

A recent *R*-matrix calculation [30] involving the topical Fe XVII ionic system has found large (orders of magnitude) enhancements in the background photoionization cross sections and huge asymmetric resonances produced by core photoexcitation, which lead to higher (35%) Rosseland means; however, such claims have been seriously questioned [31, 32, 93] [94].

B. Ni and Cr opacities

Due to their contributions to the *Z* bump, the Ni and Cr opacities have also received considerable attention. In the former case, it has been shown [21] that CI effects on the Rosseland mean are not as conspicuous as those of Fe; they manifest themselves mainly at lower photon energies (50–60 eV), but the spectral features are distinctively different from those of the OP which are believed to be faulty due to their being determined by extrapolation procedures. A similar diagnostic has been put forward for Cr and both are supported by recent transmission measurements in the XUV [33]; moreover, comparisons with data from the ATOMIC code apparently lead to discrepancies with the OP Ni Rosseland mean of a factor of 6.

V. SPECTATOR-ELECTRON PROCESSES

As mentioned in Section IV, a study of line broadening in opacity calculations has shown that the OP K-line widths are largely discrepant with those in other plasma modeling codes in conditions akin to the solar convection-zone boundary [29]. Such a finding in fact reflects essential differences in the treatment of ionic models in opacity calculations; i.e. between the OP multi-channel representations (see Fig. 1) and the simpler uncoupled, or in some cases statistical, versions adopted by other projects that become particularly conspicuous in spectator-electron processes. The latter are responsible for K-line widths, the broad profiles of resonances resulting from core photoexcitation (PECs hereafter), and ionization-edge structures.

It has been shown that the electron impact broadening of such features is intricate, requiring the contributions from the interference terms that cause overlapping lines to coalesce such that the spectator-electron relaxation does not affect the line shape, i.e. narrower lines with restricted wings [95]. Electron impact broadening of resonances in the close-coupling formalism is also currently under review [96]. Furthermore, as discussed by [26], spectator-electron transitions can give rise to a large number of X-ray satellite lines that can significantly broaden the resonance-line red wing; since they are difficult to treat in the usual detailed-line-accounting approach, the approximate statistical methods based on UTAs [82–84] previously mentioned (see Section IV) have been proposed.

In Sections V A–V C, we briefly discuss how such processes are currently handled within the *R*-matrix framework, in particular with regards to the problem of complete configuration accounting.

A. PEC resonances

PECs were first discussed in the OP by [97] and to illustrate their line shapes and widths, we consider the photoabsorption of the $3sns\ ^1S$ states of Mg-like Al II as described in [98], namely

$$3sns\ ^1S + \gamma \rightarrow 3pn's\ ^1P^o \rightarrow 3s\ ^2S + e^- . \quad (4)$$

The PEC arises when $n = n'$ whereby the ns active electron does not take place in the transition. It may be seen in Fig. 7a that the photoabsorption cross section of the Al II $3s^2$ ground state is dominated by a series of $3pn's$ asymmetric window resonances without a PEC since, for $n = n' = 3$, $3s3p$ is a true bound state below the ionization threshold. This is not the case for $3s4s\ ^1S$, the first excited state (see Fig. 7b), where now the $3p4s$ resonance lying just above the threshold becomes a huge (two orders of magnitude over the background) PEC. A similar situation occurs in the photoabsorption cross sections of the following excited states of the series, namely $3s5s$ and $3s6s$, that are respectively dominated by the $3p5s$ and $3p6s$ PECs (see Figs. 7c,d). It may be appreciated that the $3pns$ PEC widths are approximately constant and independent of the n principal quantum number since their oscillator-strength distributions are mostly determined by the $f(3s, 3p) = 0.849$ oscillator strength of the Na-like Al III core [99].

A further important point is that, to obtain the $3pns$ PECs in the photoabsorption cross sections of the $3sns$ bound-state series, it suffices to include in the close-coupling expansion of Eq. (1) the Na-like $3s$ and $3p$ core states; but, if the $4s$ and $4p$ states are additionally included, $4pns$ PECs will appear in the cross sections of the $3sns$ excited states for $n \geq 4$, whose resonance properties would be dominated by the Al III core $f(3s, 4p) = 0.0142$ oscillator strength [99]. Due to the comparatively small value of the latter, such PECs will be less conspicuous,

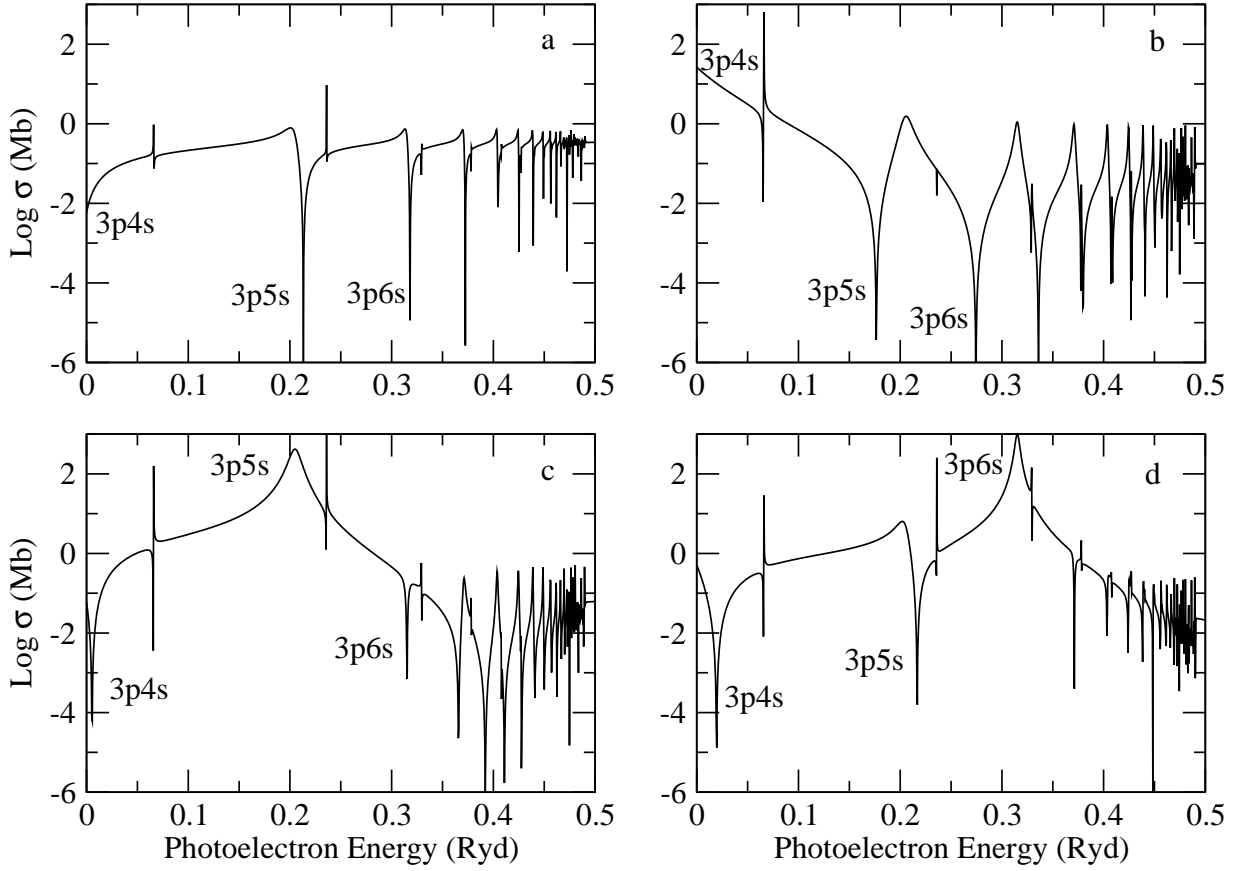


FIG. 7. Photoabsorption cross sections of the $3sns$ states of Al II showing the $3pns$ PEC resonances for $n \geq 4$. (a) $3s^2$. (b) $3s4s$. (c) $3s5s$. (d) $3s6s$.

but in systems with more complicated electron structures this will not in general be the case. In conclusion, the PEC n inventory directly depends on the n_{\max} of the CI complex of the core-state expansion in Eq. (1) whose convergence would unavoidably lead to large calculations.

B. K lines

K-resonance damping is another example of the dominance of spectator-electron processes, which can be illustrated with the photoexcitation of the ground state of Fe XVII to a K-vacancy Rydberg state

$$h\nu + 1s^22s^22p^6 \longrightarrow 1s2s^22p^6np. \quad (5)$$

This state decays via the radiative and Auger array

$$1s2s^22p^6np \xrightarrow{K\gamma} 1s^22s^22p^6 + h\nu_n \quad (6)$$

$$\xrightarrow{K\alpha} 1s^22s^22p^5np + h\nu_\alpha \quad (7)$$

$$\xrightarrow{KL\gamma} \begin{cases} 1s^22s^22p^5 + e^- \\ 1s^22s2p^6 + e^- \end{cases} \quad (8)$$

$$\xrightarrow{KLL} \begin{cases} 1s^22s^22p^4np + e^- \\ 1s^22s2p^5np + e^- \\ 1s^22p^6np + e^- \end{cases} \quad (9)$$

which has been shown to be dominated by the radiative $K\alpha$ (Eq. 7) and Auger KLL (Eq. 9) spectator-electron channels [100]. Such damping process causes the widths of the $1s2s^22p^6np$ K resonances to be broad, symmetric, and almost independent of n , leading to the smearing of the K edge as shown in Fig. 8.

An inherent difficulty of the R -matrix method is that, to properly account for the damped widths of K vacancy states such as $1s2s^22p^6np$, it implies the inclusion of the $1s^22s^22p^4np$, $1s^22s2p^5np$, and $1s^22p^6np$ core configurations of the dominant KLL channels (see Eq. 9) in the close-coupling expansion, which would rapidly make the representation of the high- n resonances as $n \rightarrow \infty$

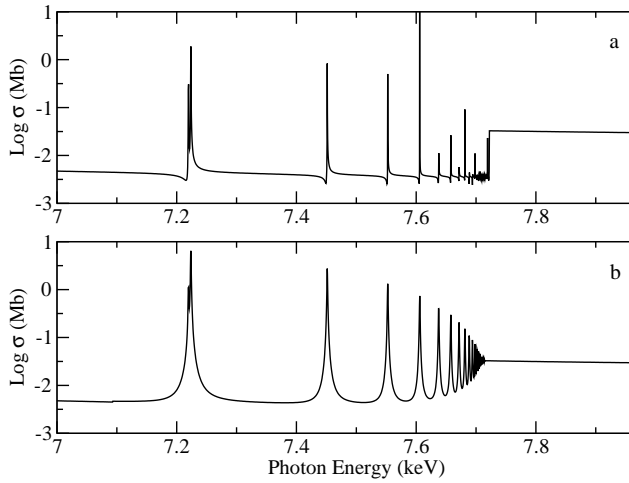


FIG. 8. Total K photoabsorption cross section of $1s^2 2s^2 2p^6 1S$ ground state of Fe XVII. (a) Undamped cross section. (b) Damped (radiation and Auger) cross section.

computationally intractable. To overcome this limitation, Auger damping is currently managed within the matrix formalism by means of an optical potential [10] which however requires the determination of the α Auger widths beforehand with an atomic structure code (e.g. AUTOSTRUCTURE). Furthermore, since K lines have such distinctive symmetric profiles, this scheme predetermining for them made-to-order damped widths to be then included in opacity calculations could also easily be implemented in perturbative methods.

Following [100], the estimated opacity of a photoionized gas with solar elemental abundances and ionization parameter $\xi = 10$ is depicted in Fig. 9 in the photon range 7–9 KeV, adopting damped and undamped cross sections. A larger number of broad peaks, particularly the $K\alpha$ transition array around 7.2 KeV, and smeared edges are key features of the former.

C. Ionization edges

While K and L ionization edges are well understood in ground-state photoabsorption cross sections in the R -matrix formalism, those for excited states have not received comparable attention. In the same way as PECs (see Section V A), the K edge arises from a spectator-electron transition whose adequate representation is limited by the n_{\max} of the core-state CI complex in the close-coupling expansion. This assertion may be illustrated using the simple O VI Li-like system as a study case.

Let us consider K photoabsorption of the $1s^2 ns$ series of this ion; the K edge occurs as

$$1s^2 ns + \gamma \longrightarrow 1s ns + e^-(kp) \quad (10)$$

where the ns electron remains a spectator in the transition; therefore, in a similar fashion to PECs, the K-edge

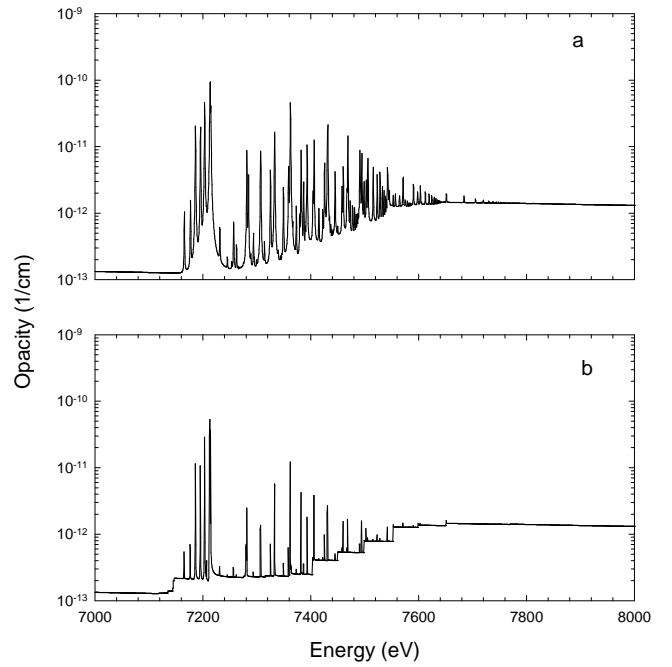


FIG. 9. Monochromatic opacity of a photoionized gas with solar abundances and ionization parameter $\xi = 10$. (a) Estimated with damped cross sections. (b) Estimated with undamped cross sections. Reproduced from Fig. 3 of Ref. [100] with permission of the ©AAS.

n -inventory would depend on the n_{\max} of the core-state representation in the close-coupling expansion (Eq. 1). In Fig. 10 the photoabsorption cross sections of these levels are plotted for $n \leq 4$ using three target representations for the He-like core —

Target A: $1s^2, 1s2\ell$ with $\ell \leq 1$

Target B: Target A plus $1s3\ell'$ with $\ell' \leq 2$

Target C: Target B plus $1s4\ell''$ with $\ell'' \leq 3$.

It may be seen that, when Target A ($n_{\max} = 2$) is implemented, a K edge appears in the photoabsorption cross section of the $1s^2 2s$ level but not in those of $1s^2 3s$ and $1s^2 4s$; for Target B where $n_{\max} = 3$, K edges are there except in the cross section of the latter; and for Target C with $n_{\max} = 4$, they are all present. As shown in Fig. 10, adequate K-edge representations for excited states are essential to obtain accurate high-energy tails in their cross sections.

Furthermore, it may be seen in Fig. 10 that, in the photoabsorption of the $1s^2 ns$ states of O VI, the strong K lines are also the result of spectator-electron transitions of the type

$$1s^2 ns + \gamma \longrightarrow 1s ns np. \quad (11)$$

That is, Target A would be sufficient to generate the $K\alpha$ lines at photoelectron energies of ~ 32 Ryd in the cross sections of the three states, but to obtain the broad

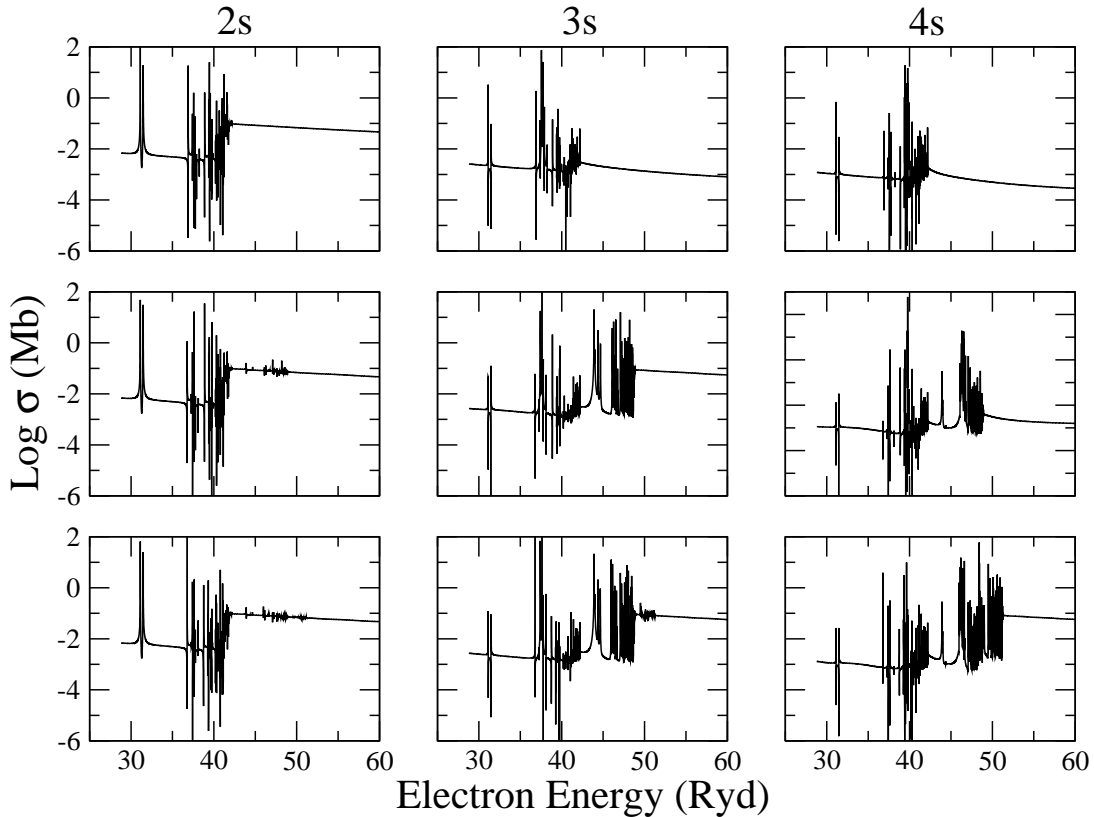


FIG. 10. K photoabsorption cross sections of the $1s^2ns$ states of O VI. Left column: 2s state. Middle column: 3s state. Right column: 4s state. First row: computed with Target A. Second row: computed with Target B. Third row: computed with Target C.

$K\beta$ transitions at ~ 44 Ryd in the $1s^23s$ cross section at least Target B is required. Target C would then be necessary to obtain the broad $K\gamma$ lines at ~ 47 Ryd in the $1s^24s$ cross section. This conclusion implies that, in the R -matrix method, satellite lines must be explicitly specified in the close-coupling expansion.

VI. CONCLUDING REMARKS

In the present review we have gone over the computational methods that were used in the earlier opacity revisions of the 1980-90s to produce fairly reliable Rosseland-mean and radiative acceleration tables that have been used to satisfactorily model a variety of astronomical entities, among them the solar interior and pulsating stars. However, more recent developments, e.g. the revision of the solar photospheric abundances and the exploitation of the powerful techniques of helio and asteroseismology, have led to a serious questioning of their accuracy.

This critical crossroads has induced extensive revisions of the opacity tables and numerical frameworks, the introduction of novel computational methods (e.g. the Super-Transition-Array method) to replace the traditional detailed-line-accounting approaches, and laboratory experiments that simulate the plasma environment

of the solar convection zone. They have certainly deepened our understanding of the contributing absorption processes but have not as yet resulted in definite missing opacities; in this respect, alternative experimental attempts to reproduce the larger-than-expected opacity measurements of [36] are currently in progress [102, 103].

Essential considerations of astrophysical opacity computations are accuracy and completeness in the treatment of the radiative absorption processes, both difficult to accomplish in spite of the powerful computational facilities available nowadays. As reviewed in Section IV, it has been shown for the topical cases of Cr, Fe, and Ni that configuration interaction (CI) effects are noticeable in the spectrum shape in certain thermodynamic regimes [16, 19, 21] while incomplete configuration accounting leads to sizable discrepancies in others [33]. To rigorously satisfy both requirements with the OP R -matrix method for isoelectronic sequences with electron number $N > 13$, it implies close-coupling expansions that soon become computationally intractable and must then be tackled with simpler CI methods (e.g. AUTOSTRUCTURE) that neglect the bound-continuum coupling. Taking into account the original satisfactory agreement between OPAL and OP as discussed in Section II C, perturbative methods such as the former appear to have an advantage in opacity calculations insofar as being able

to manage configuration accounting more exhaustively. In this respect, the introduction of powerful numerical frameworks (e.g. STA) to replace detailed line accounting reinforces this assertion. On the other hand, as discussed in Section IID, the OP R -matrix approach generates as a byproduct an atomic radiative database (e.g. TOPbase) of sufficient accuracy and completeness to be useful in a wide variety of astrophysical problems.

An inherent limitation of the OP R -matrix method in opacity calculations is that radiative properties are calculated assuming isolated atomic targets, i.e. exempt from plasma correlation effects that, as previously pointed out [104–107], could significantly modify the ionization potentials, excitation energies, and the bound–free and free–free absorption cross sections. In this respect, it has been recently shown [108] that ion–ion plasma correlations lead to $\sim 10\%$ and $\sim 15\%$ increases of the Rosseland mean opacity in the solar convection zone and in a pure iron plasma, respectively, that could be on their way to solve the solar abundance problem. Plasma inter-

actions by means of Debye–Hückel and ion-sphere potentials have already been included in atomic structure CI codes such as GRASP92 and AUTOSTRUCTURE, and are currently being used to estimate the plasma effects on the atomic parameters associated with the Fe K-vacancy states [109].

ACKNOWLEDGMENTS

I would like to thank Drs. Carlos Iglesias (Lawrence Livermore National Laboratory), James Colgan (Los Alamos National Laboratory), and Manuel Bautista (Western Michigan University) for reading the manuscript and for returning many useful suggestions that led to an improvement of its quality and scope. This work was in part supported by NASA grant 12-APRA12-0070 through the Astrophysics Research and Analysis Program.

-
- [1] P. Pismis and S. Torres-Peimbert, *Rev. Mex. Astron. Astr.* **23**, 5 (1992).
 - [2] <http://cdsweb.u-strasbg.fr/topbase/TheOP.html>.
 - [3] <http://opalopacity.llnl.gov/opal.html>.
 - [4] N. R. Simon, *Astrophys. J.* **260**, L87 (1982).
 - [5] A. N. Cox and J. E. Tabor, *Astrophys. J. Suppl. S.* **31**, 271 (1976).
 - [6] N. R. Badnell, M. A. Bautista, K. Butler, F. Delahaye, C. Mendoza, P. Palmeri, C. J. Zeippen, and M. J. Seaton, *Mon. Not. R. Astron. Soc.* **360**, 458 (2005), [astro-ph/0410744](https://arxiv.org/abs/astro-ph/0410744).
 - [7] M. Asplund, N. Grevesse, and A. J. Sauval, in *Cosmic Abundances as Records of Stellar Evolution and Nucleosynthesis*, Astronomical Society of the Pacific Conference Series, Vol. 336, edited by T. G. Barnes, III and F. N. Bash (2005) p. 25.
 - [8] J. N. Bahcall, S. Basu, M. Pinsonneault, and A. M. Serenelli, *Astrophys. J.* **618**, 1049 (2005), [astro-ph/0407060](https://arxiv.org/abs/astro-ph/0407060).
 - [9] J. N. Bahcall, A. M. Serenelli, and S. Basu, *Astrophys. J.* **621**, L85 (2005), [astro-ph/0412440](https://arxiv.org/abs/astro-ph/0412440).
 - [10] E. Caffau, H.-G. Ludwig, M. Steffen, B. Freytag, and P. Bonifacio, *Sol. Phys.* **268**, 255 (2011), [arXiv:1003.1190 \[astro-ph.SR\]](https://arxiv.org/abs/1003.1190).
 - [11] F. Jin, J. Zeng, T. Huang, Y. Ding, Z. Zheng, and J. Yuan, *Astrophys. J.* **693**, 597 (2009).
 - [12] D. Gilles, S. Turck-Chièze, G. Loisel, L. Piau, J.-E. Ducret, M. Poirier, T. Blenski, F. Thais, C. Blancard, P. Cossé, G. Faussurier, F. Gilleron, J. C. Pain, Q. Porcherot, J. A. Guzik, D. P. Kilcrease, N. H. Magee, J. Harris, M. Busquet, F. Delahaye, C. J. Zeippen, and S. Bastiani-Ceccotti, *High Energy Den. Phys.* **7**, 312 (2011), [arXiv:1201.6245 \[astro-ph.SR\]](https://arxiv.org/abs/1201.6245).
 - [13] S. N. Nahar, A. K. Pradhan, G.-X. Chen, and W. Eissner, *Phys. Rev. A* **83**, 053417 (2011), [arXiv:1104.2881 \[astro-ph.SR\]](https://arxiv.org/abs/1104.2881).
 - [14] S. Turck-Chièze, G. Loisel, D. Gilles, L. Piau, C. Blancard, T. Blenski, M. Busquet, T. Caillaud, P. Cossé, F. Delahaye, G. Faussurier, J. Fariaut, F. Gilleron, J. A. Guzik, J. Harris, D. P. Kilcrease, N. H. Magee, J. C. Pain, Q. Porcherot, M. Poirier, G. Soullier, C. J. Zeippen, S. Bastiani-Ceccotti, C. Reverdin, V. Silvert, F. Thais, and B. Villette, *Astrophys. Space Sci.* **336**, 103 (2011), [arXiv:1101.1170 \[astro-ph.SR\]](https://arxiv.org/abs/1101.1170).
 - [15] C. Blancard, P. Cossé, and G. Faussurier, *Astrophys. J.* **745**, 10 (2012).
 - [16] D. Gilles, S. Turck-Chièze, M. Busquet, F. Thais, G. Loisel, L. Piau, J. E. Ducret, T. Blenski, M. Poirier, C. Blancard, P. Cossé, G. Faussurier, F. Gilleron, J. C. Pain, J. A. Guzik, D. P. Kilcrease, N. H. Magee, J. Harris, S. Bastiani-Ceccotti, F. Delahaye, and C. J. Zeippen, in *EAS Publications Series*, EAS Publications Series, Vol. 58, edited by C. Stehlé, C. Joblin, and L. d’Hendecourt (2012) pp. 51–55.
 - [17] M. Busquet, M. Klapisch, and D. Gilles, in *European Physical Journal Web of Conferences*, European Physical Journal Web of Conferences, Vol. 59 (2013) p. 14004.
 - [18] F. Delahaye, P. Palmeri, P. Quinet, and C. J. Zeippen, in *EAS Publications Series*, EAS Publications Series, Vol. 63, edited by G. Alecian, Y. Lebreton, O. Richard, and G. Vauclair (2013) pp. 321–330.
 - [19] D. Gilles, S. Turck-Chièze, M. Busquet, F. Thais, G. Loisel, L. Piau, J. E. Ducret, T. Blenski, C. Blancard, P. Cossé, G. Faussurier, F. Gilleron, J. C. Pain, Q. Porcherot, J. A. Guzik, D. P. Kilcrease, N. H. Magee, J. Harris, S. Bastiani-Ceccotti, F. Delahaye, and C. J. Zeippen, in *European Physical Journal Web of Conferences*, European Physical Journal Web of Conferences, Vol. 59 (2013) p. 14003, [arXiv:1201.4692 \[astro-ph.SR\]](https://arxiv.org/abs/1201.4692).
 - [20] S. Turck-Chièze, D. Gilles, F. Gilleron, and J. C. Pain, in *SF2A-2013: Proceedings of the Annual meeting of the French Society of Astronomy and Astrophysics*, edited

- by L. Cambresy, F. Martins, E. Nuss, and A. Palacios (2013) pp. 105–110.
- [21] S. Turck-Chièze, D. Gilles, M. Le Pennec, T. Blenski, F. Thais, S. Bastiani-Ceccotti, C. Blancard, M. Busquet, T. Caillaud, J. Colgan, P. Cossé, F. Delahaye, J. E. Ducreta, G. Faussurier, C. J. Fontes, F. Gilleron, J. Guzik, J. W. Harris, D. P. Kilcrease, G. Loisel, N. H. Magee, J. C. Pain, C. Reverdin, V. Silvert, B. Villette, and C. J. Zeippen, *High Energy Den. Phys.* **9**, 473 (2013).
- [22] S. Turck-Chièze and D. Gilles, in *European Physical Journal Web of Conferences*, European Physical Journal Web of Conferences, Vol. 43 (2013) p. 01003.
- [23] C. J. Fontes, C. L. Fryer, A. L. Hungerford, P. Hakel, J. Colgan, D. P. Kilcrease, and M. E. Sherrill, *High Energy Den. Phys.* **16**, 53 (2015).
- [24] C. A. Iglesias, *Mon. Not. R. Astron. Soc.* **450**, 2 (2015).
- [25] G. Mondet, C. Blancard, P. Cossé, and G. Faussurier, *Astrophys. J. Suppl. S.* **220**, 2 (2015).
- [26] J.-C. Pain and F. Gilleron, *High Energy Den. Phys.* **15**, 30 (2015), arXiv:1503.08939 [physics.atom-ph].
- [27] M. Le Pennec, S. Turck-Chièze, S. Salmon, C. Blancard, P. Cossé, G. Faussurier, and G. Mondet, *Astrophys. J.* **813**, L42 (2015), arXiv:1510.05600 [astro-ph.SR].
- [28] M. Krief, A. Feigel, and D. Gazit, *Astrophys. J.* **821**, 45 (2016), arXiv:1601.01930 [astro-ph.SR].
- [29] M. Krief, A. Feigel, and D. Gazit, *Astrophys. J.* **824**, 98 (2016), arXiv:1603.01153 [astro-ph.SR].
- [30] S. N. Nahar and A. K. Pradhan, *Phys. Rev. Lett.* **116**, 235003 (2016), arXiv:1606.02731 [astro-ph.SR].
- [31] C. Blancard, J. Colgan, P. Cossé, G. Faussurier, C. J. Fontes, F. Gilleron, I. Golovkin, S. B. Hansen, C. A. Iglesias, D. P. Kilcrease, J. J. MacFarlane, R. M. More, J.-C. Pain, M. Sherrill, and B. G. Wilson, *Phys. Rev. Lett.* **117**, 249501 (2016), arXiv:1608.03512 [physics.atom-ph].
- [32] S. N. Nahar and A. K. Pradhan, *Phys. Rev. Lett.* **117**, 249502 (2016).
- [33] S. Turck-Chièze, M. Le Pennec, J. E. Ducret, J. Colgan, D. P. Kilcrease, C. J. Fontes, N. Magee, F. Gilleron, and J. C. Pain, *Astrophys. J.* **823**, 78 (2016).
- [34] <http://aphysics2.lanl.gov/opacity/lanl/>.
- [35] J. Colgan, D. P. Kilcrease, N. H. Magee, M. E. Sherrill, J. Abdallah, Jr., P. Hakel, C. J. Fontes, J. A. Guzik, and K. A. Mussack, *Astrophys. J.* **817**, 116 (2016), arXiv:1601.01005 [astro-ph.SR].
- [36] J. E. Bailey, T. Nagayama, G. P. Loisel, G. A. Rochau, C. Blancard, J. Colgan, P. Cosse, G. Faussurier, C. J. Fontes, F. Gilleron, I. Golovkin, S. B. Hansen, C. A. Iglesias, D. P. Kilcrease, J. J. MacFarlane, R. C. Mancini, S. N. Nahar, C. Orban, J.-C. Pain, A. K. Pradhan, M. Sherrill, and B. G. Wilson, *Nature* **517**, 56 (2015).
- [37] J. Daszyńska-Daszkiewicz and P. Walczak, *Mon. Not. R. Astron. Soc.* **403**, 496 (2010), arXiv:0912.0622 [astro-ph.SR].
- [38] K. A. Berrington, P. G. Burke, K. Butler, M. J. Seaton, P. J. Storey, K. T. Taylor, and Y. Yan, *J. Phys. B - At. Mol.* **20**, 6379 (1987).
- [39] W. Eissner, M. Jones, and H. Nussbaumer, *Comput. Phys. Commun.* **8**, 270 (1974).
- [40] A. Hibbert, *Comput. Phys. Commun.* **9**, 141 (1975).
- [41] P. G. Burke, A. Hibbert, and W. D. Robb, *J. Phys. B - At. Mol.* **4**, 153 (1971).
- [42] K. A. Berrington, W. B. Eissner, and P. H. Norrington, *Comput. Phys. Commun.* **92**, 290 (1995).
- [43] M. J. Seaton, *J. Phys. B - At. Mol.* **19**, 2601 (1986).
- [44] F. J. Rogers, B. G. Wilson, and C. A. Iglesias, *Phys. Rev. A* **38**, 5007 (1988).
- [45] C. A. Iglesias, F. J. Rogers, and B. G. Wilson, *Rev. Mex. Astron. Astr.* **23**, 133 (1992).
- [46] D. G. Hummer and D. Mihalas, *Astrophys. J.* **331**, 794 (1988).
- [47] D. Mihalas, *Rev. Mex. Astron. Astr.* **23**, 127 (1992).
- [48] F. J. Rogers and C. A. Iglesias, *Rev. Mex. Astron. Astr.* **23**, 133 (1992).
- [49] C. A. Iglesias, F. J. Rogers, and B. G. Wilson, *Astrophys. J.* **322**, L45 (1987).
- [50] A. E. Lynas-Gray, M. J. Seaton, and P. J. Storey, *J. Phys. B - At. Mol.* **28**, 2817 (1995).
- [51] L. B. da Silva, B. J. MacGowan, D. R. Kania, B. A. Hammel, C. A. Back, E. Hsieh, R. Doyas, C. A. Iglesias, F. J. Rogers, and R. W. Lee, *Phys. Rev. Lett.* **69**, 438 (1992).
- [52] C. A. Iglesias and F. J. Rogers, *Astrophys. J.* **443**, 460 (1995).
- [53] N. R. Badnell and M. J. Seaton, *J. Phys. B - At. Mol.* **36**, 4367 (2003), astro-ph/0308393.
- [54] M. J. Seaton and N. R. Badnell, *Mon. Not. R. Astron. Soc.* **354**, 457 (2004), astro-ph/0404437.
- [55] S. M. Kanbur and N. R. Simon, *Astrophys. J.* **420**, 880 (1994).
- [56] T. Hey, S. Tansley, and K. Tolle, eds., *The Fourth Paradigm: Data-Intensive Scientific Discovery* (Microsoft Research, Redmond, Washington, 2009).
- [57] W. Cunto and C. Mendoza, *Rev. Mex. Astron. Astr.* **23**, 107 (1992).
- [58] W. Cunto, C. Mendoza, F. Ochsenbein, and C. J. Zeippen, *Astron. Astrophys.* **275**, L5 (1993).
- [59] <http://cdsweb.u-strasbg.fr/>.
- [60] C. Mendoza, M. J. Seaton, P. Buerger, A. Bellorín, M. Meléndez, J. González, L. S. Rodríguez, F. Delahaye, E. Palacios, A. K. Pradhan, and C. J. Zeippen, *Mon. Not. R. Astron. Soc.* **378**, 1031 (2007), arXiv:0704.1583.
- [61] <https://www.osc.edu/>.
- [62] J. Christensen-Dalsgaard, M. P. di Mauro, G. Houdek, and F. Pijpers, *Astron. Astrophys.* **494**, 205 (2009), arXiv:0811.1001.
- [63] S. Basu and H. M. Antia, *Astrophys. J.* **606**, L85 (2004), astro-ph/0403485.
- [64] N. Grevesse and A. J. Sauval, *Space Sci. Rev.* **85**, 161 (1998).
- [65] S. Turck-Chièze, *J. Phys. - Conf. Ser.* **665**, 012078 (2016).
- [66] R. von Steiger and T. H. Zurbuchen, *Astrophys. J.* **816**, 13 (2016).
- [67] A. Serenelli, P. Scott, F. L. Villante, A. C. Vincent, M. Asplund, S. Basu, N. Grevesse, and C. Peña-Garay, *Mon. Not. R. Astron. Soc.* **463**, 2 (2016), arXiv:1604.05318 [astro-ph.SR].

- [68] M. Asplund, N. Grevesse, A. J. Sauval, and P. Scott, *Annu. Rev. Astron. Astr.* **47**, 481 (2009), arXiv:0909.0948 [astro-ph.SR].
- [69] A. M. Serenelli, S. Basu, J. W. Ferguson, and M. Asplund, *Astrophys. J.* **705**, L123 (2009), arXiv:0909.2668 [astro-ph.SR].
- [70] A. Serenelli, *Eur. Phys. J. A* **52**, 78 (2016), arXiv:1601.07179 [astro-ph.SR].
- [71] E. G. Adelberger, A. García, R. G. H. Robertson, K. A. Snover, A. B. Balantekin, K. Heeger, M. J. Ramsey-Musolf, D. Bemmerer, A. Junghans, C. A. Bertulani, J.-W. Chen, H. Costantini, P. Prati, M. Couder, E. Uberseder, M. Wiescher, R. Cyburt, B. Davids, S. J. Freedman, M. Gai, D. Gazit, L. Gialanella, G. Imbriani, U. Greife, M. Hass, W. C. Haxton, T. Itahashi, K. Kubodera, K. Langanke, D. Leitner, M. Leitner, P. Vetter, L. Winslow, L. E. Marcucci, T. Motobayashi, A. Mukhamedzhanov, R. E. Tribble, K. M. Nollett, F. M. Nunes, T.-S. Park, P. D. Parker, R. Schiavilla, E. C. Simpson, C. Spitaleri, F. Strieder, H.-P. Trautvetter, K. Suemmerer, and S. Typel, *Rev. Mod. Phys.* **83**, 195 (2011), arXiv:1004.2318 [nucl-ex].
- [72] S. V. Vorontsov, V. A. Baturin, S. V. Ayukov, and V. K. Gryaznov, *Mon. Not. R. Astron. Soc.* **430**, 1636 (2013).
- [73] <http://kepler.nasa.gov/>.
- [74] <http://bit.ly/2cYJ09w>.
- [75] W. J. Chaplin and A. Miglio, *Annu. Rev. Astron. Astr.* **51**, 353 (2013), arXiv:1303.1957 [astro-ph.SR].
- [76] P. Walczak and J. Daszyńska-Daszkiewicz, *Astron. Nachr.* **331**, 1057 (2010), arXiv:1004.2366 [astro-ph.SR].
- [77] J. A. Guzik, C. J. Fontes, P. Walczak, S. R. Wood, K. Mussack, and E. Farag, *ArXiv e-prints* (2016), arXiv:1605.04452 [astro-ph.SR].
- [78] P. Walczak, C. J. Fontes, J. Colgan, D. P. Kilcrease, and J. A. Guzik, *Astron. Astrophys.* **580**, L9 (2015).
- [79] J. Daszyńska-Daszkiewicz, A. A. Pamyatnykh, P. Walczak, J. Colgan, C. J. Fontes, and D. P. Kilcrease, *ArXiv e-prints* (2016), arXiv:1612.05820 [astro-ph.SR].
- [80] F. Delahaye, C. M. Zwölf, C. J. Zeippen, and C. Mendoza, *J. Quant. Spectrosc. Ra.* **171**, 66 (2016), arXiv:1511.07260 [astro-ph.SR].
- [81] J. Bauche, C. Bauche-Arnoult, and M. Klapisch, *Phys. Scripta* **37**, 659 (1988).
- [82] C. A. Iglesias and V. Sonnad, *High Energy Den. Phys.* **8**, 154 (2012).
- [83] C. A. Iglesias, *High Energy Den. Phys.* **8**, 260 (2012).
- [84] C. A. Iglesias, *High Energy Den. Phys.* **8**, 253 (2012).
- [85] G. Hazak and Y. Kurzweil, *High Energy Den. Phys.* **8**, 290 (2012), arXiv:1204.2896 [physics.atom-ph].
- [86] B. G. Wilson, C. A. Iglesias, and M. H. Chen, *High Energy Den. Phys.* **14**, 67 (2015).
- [87] Y. Kurzweil and G. Hazak, *Phys. Rev. E* **94**, 053210 (2016).
- [88] T. Nagayama, J. E. Bailey, R. C. Mancini, C. A. Iglesias, S. B. Hansen, C. Blancard, H. K. Chung, J. Colgan, P. Cosse, G. Faussurier, R. Florido, C. J. Fontes, F. Gilleron, I. E. Golovkin, D. P. Kilcrease, G. Loisel, J. J. MacFarlane, J.-C. Pain, G. A. Rochau, M. E. Sherrill, and R. W. Lee, *High Energy Den. Phys.* **20**, 17 (2016).
- [89] C. A. Iglesias and F. J. Rogers, *Astrophys. J.* **371**, 408 (1991).
- [90] A. Bar-Shalom, M. Klapisch, and J. Oreg, *J. Quant. Spectrosc. Ra.* **71**, 169 (2001).
- [91] J. E. Bailey, G. A. Rochau, C. A. Iglesias, J. Abdallah, Jr., J. J. Macfarlane, I. Golovkin, P. Wang, R. C. Mancini, P. W. Lake, T. C. Moore, M. Bump, O. Garcia, and S. Mazevet, *Phys. Rev. Lett.* **99**, 265002 (2007).
- [92] C. A. Iglesias, *High Energy Den. Phys.* **15**, 4 (2015).
- [93] C. A. Iglesias and S. B. Hansen, *Astrophys. J.* **835**, 284 (2017).
- [94] A. K. Pradhan, private communication (2017).
- [95] C. A. Iglesias, *High Energy Den. Phys.* **6**, 318 (2010).
- [96] A. K. Pradhan, private communication (2016).
- [97] Y. Yan and M. J. Seaton, *J. Phys. B - At. Mol.* **20**, 6409 (1987).
- [98] K. Butler, C. Mendoza, and C. J. Zeippen, *J. Phys. B - At. Mol.* **26**, 4409 (1993).
- [99] K. Butler, C. Mendoza, and C. J. Zeippen, *J. Phys. B - At. Mol.* **17**, 2039 (1984).
- [100] P. Palmeri, C. Mendoza, T. R. Kallman, and M. A. Bautista, *Astrophys. J.* **577**, L119 (2002), astro-ph/0207324.
- [101] T. W. Gorczyca and F. Robicheaux, *Phys. Rev. A* **60**, 1216 (1999).
- [102] B. Qing, Y. Zhao, M.-X. Wei, H. Li, G. Xiong, M. Lv, Z.-M. Hu, J.-Y. Zhang, and J.-M. Yang, *Chin. Phys. Lett.* **33**, 035203 (2016).
- [103] P. W. Ross, R. F. Heeter, M. F. Ahmed, E. Dodd, E. J. Huffman, D. A. Liedahl, J. A. King, Y. P. Opachich, M. B. Schneider, and T. S. Perry, *Rev. Sci. Instrum.* **87**, 11D623 (2016).
- [104] B. F. Rozsnyai, *Phys. Rev. A* **43**, 3035 (1991).
- [105] T. N. Chang and T. K. Fang, *Phys. Rev. A* **88**, 023406 (2013).
- [106] M. Belkhiri, C. J. Fontes, and M. Poirier, *Phys. Rev. A* **92**, 032501 (2015).
- [107] M. Das, B. K. Sahoo, and S. Pal, *Phys. Rev. A* **93**, 052513 (2016), arXiv:1604.01735 [physics.plasm-ph].
- [108] M. Krief, Y. Kurzweil, A. Feigel, and D. Gazit, *ArXiv e-prints* (2016), arXiv:1611.09339 [astro-ph.SR].
- [109] J. Deprince, S. Fritzsche, T. Kallman, P. Palmeri, and P. Quinet, *ArXiv e-prints* (2017), arXiv:1701.05757 [physics.atom-ph].